Anomalous Hall Coulomb drag of massive Dirac fermions

Hong Liu, Weizhe Edward Liu, and Dimitrie Culcer

School of Physics, The University of New South Wales, Sydney 2052, Australia

Dirac fermions have been actively investigated in recent years, both theoretically and experimentally. Some materials hosting Dirac fermions are natural platforms for interlayer coherence effects such as Coulomb drag and exciton condensation. Here we determine the role played by the anomalous Hall effect in Coulomb drag in *doped* massive Dirac fermion systems. We focus on topological insulator films with out-of plane magnetizations in *both* the active and passive layers. The transverse response of the active layer is dominated by a topological term arising from the Berry curvature. We show that the topological mechanism does not contribute to Coulomb drag, yet the longitudinal drag force in the passive layer gives rise to a transverse drag current. This anomalous Hall drag current is independent of the active-layer magnetization, a fact that can be verified experimentally. It depends nonmonotonically on the passive-layer magnetization, exhibiting a peak that becomes more pronounced at low densities. These findings are expected to stimulate new experiments and quantitative studies of anomalous Hall drag.

I. INTRODUCTION

The past decade has witnessed an energetic exploration of Dirac fermions in materials ranging from graphene [1] to topological insulators [2], transition metal dichalcogenides [3], and Weyl and Dirac semimetals [4–6]. Dirac fermions in two dimensions are described by the Hamiltonian $H_D = A\,\boldsymbol{\sigma} \cdot (\boldsymbol{k} \times \hat{\boldsymbol{z}}) + M\sigma_z$, with $\boldsymbol{\sigma} = (\sigma_x, \sigma_y, \sigma_z)$ the usual Pauli matrices, $\boldsymbol{k} = (k_x, k_y)$ the 2D wave vector, A stems from the Fermi velocity, and M a generic mass term. In the limit $M \to 0$ the quasiparticle dispersion is linear, a feature that has aroused intense interest experimentally [7–21] and theoretically [22–34]. Recent studies have illuminated the considerable potential of Dirac fermions for spintronics [35] and topological quantum computing [36].

Certain materials hosting Dirac fermions, such as 3D topological insulator (TI) slabs, are inherently two-layer systems naturally exhibiting interlayer coherence effects such as Coulomb drag [37,38], in which the charge current in one layer *drags* a charge current in the adjacent layer through the interlayer electron-electron interactions. Drag geometries are intensively studied experimentally and theoretically in semiconductor and Dirac fermion systems as part of the search for exciton condensation [39–69]. The most promising Dirac fermion materials have been magnetic TI slabs, in which a dissipationless quantized anomalous Hall effect has been discovered [70–73], which has already been harnessed successfully [74], stimulating an intense search for device applications. The time-reversal symmetry breaking required in Hall effects [3,28,75–78] gives Dirac fermions a finite mass and results in a nontrivial Berry curvature [3,79,80]. Coulomb drag of massive Dirac fermions is thus directly relevant to ongoing experiments and raises important questions: If topological terms are present in the drag current they could be exploited in longitudinal transport, potentially enabling a topological transistor.

In this paper we present a complete theory of Coulomb drag of massive Dirac fermions, focusing on the role of the anomalous Hall contributions to the drag current. As a model example we will consider the surface states of 3D topological insulators in which an out of plane magnetization exists (but no magnetic field). The central finding of our work is that the (topological) anomalous Hall current in the active layer does not generate a drag current at all in the passive layer. In addition, the anomalous Hall drag current is quite generally independent of the active-layer magnetization M_a, and only depends on M_p, the magnetization of the passive layer. The dependence on M_p is nonmonotonic, with a peak at an intermediate value of M_p, which becomes pronounced at low densities.

The physical understanding of these findings is as follows. We recall that in a Coulomb drag setup an external electric field drives the electrons in the active layer longitudinally, and these in turn exert a longitudinal drag force on the passive-layer electrons. The drag force acts as an effective longitudinal driving term for the passive-layer electrons, which is responsible for the customary longitudinal drag current. The electric field also generates an anomalous Hall current in the active layer. This response is dominated by topological terms of the order of the conductivity quantum, which represents a re-arrangement of charge carriers among spin-momentum locked energy states. In other words, the anomalous Hall effect in the active layer arises as a result of the topological monopole structure around the origin in reciprocal space associated with the Rashba spin-orbit interaction. This by itself does not lead to a drag effect, since Coulomb drag occurs as a result of the interaction between the nonequilibrium charge densities in different layers, whereas *the anomalous Hall current flowing in the active layer is not associated with a change in the charge density*: It does not arise from a shift in the Fermi surface but from the Berry phase acquired by the conduction electrons. The surviving anomalous Hall component of the drag current, which at low temperatures can be sizable compared to the longitudinal component, represents the transverse response of the passive layer to the effective longitudinal driving force, and consequently depends on the passive-layer magnetization M_p.

Although derived here using a minimal model for Dirac fermions, the results we report apply generally to materials with Rashba spin-orbit interactions. They stand in sharp contrast to conventional Coulomb drag in ordinary Hall

systems [48,60,62,66,81–84]. There the Hall current in the active layer, caused by the Lorentz force rather than topology, makes a significant contribution to the longitudinal and Hall drag response, which depends on the applied magnetic field. This work is intended to stimulate further experiments and quantitative studies on state-of-the-art samples, in which the above results can be verified.

The outline of this paper is as follows. The Hamiltonian of the system is introduced in Sec. II, while in Sec. III a description of the general formalism is given, including the full interlayer electron-electron scattering term, which is the term ultimately responsible for Coulomb drag, including the interlayer dynamical screened Coulomb interaction. In Sec. IV, we derive the kinetic equation of magnetic topological insulators for spin density matrices of top and bottom surfaces with the full scattering term in the presence of an arbitrary elastic scattering potential to linear order in the impurity density. In Sec. V, we calculate the different contributions to the drag current separately, while Sec. VI discusses the broader implications of our results and possibilities for experimental observation. Our findings are summarized in Sec. VII.

II. HAMILTONIAN

We consider a model system comprised of a TI film with both the top (active) and bottom (passive) surfaces magnetized either through doping with magnetic impurities or proximity coupling to ferromagnets. The magnetizations of the two surfaces are allowed to differ. The chemical potential lies in the surface conduction band of each layer. We require $\varepsilon_F \tau_l / \hbar \gg 1$ in each layer $l \in \{a \equiv \text{active}, p \equiv \text{passive}\}$, with ε_F the Fermi energy located in the surface conduction bands and τ_l the momentum scattering time. Without loss of generality we assume (i) the carrier number density and hence the Fermi energy is the same in each layer and (ii) sidewall states do not participate in transport, an assumption that recent work has shown to be justified at large doping [85]. The two-layer effective band Hamiltonian

$$H_{0\boldsymbol{k}} = \tau_z \otimes h_{\boldsymbol{k}} + \text{diag}\{M_a, -M_a, M_p, -M_p\}, \qquad (1)$$

where the (Rashba) Hamiltonian of a single layer $h_{\boldsymbol{k}} = A\boldsymbol{\sigma} \cdot (\boldsymbol{k} \times \hat{\boldsymbol{z}}) \equiv -Ak\boldsymbol{\sigma} \cdot \hat{\boldsymbol{\theta}}$ with $\hat{\boldsymbol{\theta}}$ the tangential unit vector corresponding to $\boldsymbol{k}$. The Pauli matrix τ_z represents the layer degree of freedom. The eigenvalues of Eq. (1) are $\varepsilon_{l\pm} = \pm\sqrt{A^2 k^2 + M_l^2} \equiv \hbar \Omega_k^{(l)}$, the band index $s_{\boldsymbol{k}} = \pm$ with $+$ the conduction band and $-$ the valence band. We choose the unit vectors $\hat{\boldsymbol{\Omega}}_{\boldsymbol{k}} = -a_k \hat{\boldsymbol{\theta}} + b_k \hat{\boldsymbol{z}}, \hat{\boldsymbol{k}}_{\text{eff}} = \hat{\boldsymbol{k}}$ and $\hat{\boldsymbol{z}}_{\text{eff}} = a_k \hat{\boldsymbol{z}} + b_k \hat{\boldsymbol{\theta}}$, with $a_k = 2Ak/\hbar\Omega_k, b_k = 2M_l/\hbar\Omega_k$ so that $a_k^2 + b_k^2 = 1$ (we suppress the layer indices in a_k, b_k for simplicity). Although magnetic impurities also cause spin-dependent scattering, our recent work showed that the anomalous Hall effect in TIs is dominated by the band structure spin-orbit coupling, hence we do not include explicitly spin-dependent scattering due to any potential magnetic impurities [28].

The single-particle Hamiltonian $\hat{H}^{1e} = \hat{H}_0 + \hat{H}_E + \hat{U}$, where $\hat{H}_0$ is the band Hamiltonian defined in Eq. (1), $\hat{H}_E = e(\hat{\boldsymbol{E}} \otimes \mathbb{1}) \cdot \hat{\boldsymbol{r}}$ is the electrostatic potential due to the driving electric field with $\hat{\boldsymbol{r}}$ the position operator and $\hat{U}$ the disorder potential, which is assumed to be a scalar in spin space. Adding the two-particle interaction term we write the total Hamiltonian

as $\hat{H} = \hat{H}^{1e} + \hat{V}^{ee}$ with the single-particle term expressed generically as $\hat{H}^{1e} = \sum_{\alpha\beta} H_{\alpha\beta} c_\alpha^\dagger c_\beta$ and the Coulomb interaction term $\hat{V}^{ee} = \frac{1}{2} \sum_{\alpha\beta\gamma\delta} V_{\alpha\beta\gamma\delta}^{ee} c_\alpha^\dagger c_\beta^\dagger c_\gamma c_\delta$. The indices $\alpha \equiv \boldsymbol{k} s_{\boldsymbol{k}} l$ represent wave vector, band, and layer indices, respectively. The matrix element $V_{\alpha\beta\gamma\delta}^{ee}$ in a generic basis $\{\phi_\alpha(\boldsymbol{r})\}$ is given by $V_{\alpha\beta\gamma\delta}^{ee} = \int d\boldsymbol{r} \int d\boldsymbol{r}' \, \phi_\alpha^*(\boldsymbol{r}) \phi_\beta^*(\boldsymbol{r}') V_{\boldsymbol{r}-\boldsymbol{r}'}^{ee} \phi_\delta(\boldsymbol{r}) \phi_\gamma(\boldsymbol{r}')$, where $V_{\boldsymbol{r}-\boldsymbol{r}'}^{ee}$ is the Coulomb interaction in real space.

Electrons in magnetic TIs experience a combination of a momentum-dependent Rashba-type effective magnetic field and a magnetization perpendicular to the surface. When an electric field is applied, during electron-electron scattering processes, due to the Coulomb interactions and spin structure of the Hamiltonian, the spins of electrons in one layer are rotated while they scatter off electrons in the other layer.

III. GENERAL FORMALISM

The effects discussed in this work are driven by the electrons in the surface conduction band(s) of a topological insulator. Our aim is to elucidate the physical origins and roles of the different contributions to the Hall component of the drag current in the passive layer in a magnetic topological insulator, which exhibits the anomalous Hall effect. Given the interplay of several mechanisms the situation is relatively complex.

In a nonmagnetic system the physics of Coulomb drag is transparent. A longitudinal current in the active layer *drags* with it a longitudinal current in the passive layer. In the active layer the picture is simple—the applied electric field accelerates electrons, while collisions involving impurities and phonons keep the Fermi surface near equilibrium. In a magnetic system on the other hand the current in the active layer will have a longitudinal and a Hall component, the latter being a result of the anomalous Hall effect. The principal mechanisms behind the anomalous Hall effect are [75]: (i) a topological mechanism related to spin precession under the combined action of spin-orbit coupling and the external electric field, which is strongly renormalized by scalar scattering (ii) three spin-dependent scattering mechanisms, which were shown to be of secondary importance in TIs. Scalar disorder renormalizations affecting (i) are fully taken into account in our density matrix theory, and in this work we do not take into account the spin dependent scattering mechanisms, whose contributions are far smaller. The mechanism leading to the anomalous Hall effect in this work is therefore topological, and is very different in nature to the mechanism leading to the longitudinal current. In topological insulators this mechanism can make a sizable contribution, with anomalous Hall conductivities of the order of the conductivity quantum.

Likewise, the drag current in a magnetic system will have a longitudinal component and a Hall component, which can be measured separately. If we regard the current in the active layer as giving rise to an effective drag force, it is natural to ask which components of this drag force make the most sizable contribution to the drag current. Indeed, if we focus on the Hall component of the drag current we identify two potential contributions having physically distinct origins. Firstly, the longitudinal current in the active layer can give rise to a *transverse drag force* in the passive layer, resulting in a Hall current. Secondly, the Hall current in the active layer,

stemming from a topological mechanism, can itself directly drag a Hall current in the passive layer, in what may be termed *direct Hall drag*. Since these contributions appear as a result of different physical processes we calculate them separately in this work.

It is well known that the undoped limit of a magnetic topological insulator is a special case [28]. When the chemical potential lies in the middle of the gap opened by the magnetization between the surface conduction and valence bands the anomalous Hall conductivity is quantized: In three dimensions a single TI surface contributes exactly $e^2/(2h)$ to the Hall conductivity, referred to as the quantized anomalous Hall effect (QAHE). In a doped system the QAHE effectively yields an offset to the measured anomalous Hall conductivity. In the work presented here the QAHE emerges naturally as the special case in which the carrier density in the conduction band is taken to zero. We discuss this special case at the end of our exposition, yet we wish to stress that it does not constitute the focus of our work. However, the results we find concerning the QAHE contribution to drag based on our 2D model are also supported by an alternative picture of the QAHE based on edge states, which we discuss briefly below. Again, we emphasize that any reference to edge states is only physically meaningful at *zero doping* and only applies to the special case of the QAHE.

A. Many-body density matrix

The two-layer system is described by an effective two-dimensional model. The many-body density matrix $\hat{F}$ obeys the quantum Liouville equation [86]

$$\frac{d\hat{F}}{dt} + \frac{i}{\hbar}[\hat{H}, \hat{F}] = 0. \quad (2)$$

The one-particle reduced density matrix is the trace $\text{tr}(c_\eta^\dagger c_\xi \hat{F}) \equiv \langle c_\eta^\dagger c_\xi \rangle$. Its $\boldsymbol{k}$-diagonal part can be written as a 4×4 matrix in the joint spin/layer pseudo-spin subspace, and we refer to this matrix as $f_{\boldsymbol{k}}$. To second order in the electron-electron interaction, $f_{\boldsymbol{k}}$ satisfies [87]

$$\frac{df_{\boldsymbol{k}}}{dt} + \frac{i}{\hbar}[H^{1e}, f_{\boldsymbol{k}}] + \hat{J}_{ee}(f_{\boldsymbol{k}}) = 0. \quad (3)$$

The term $\hat{J}_{ee}(f_{\boldsymbol{k}})$ in Eq. (3) represents intralayer and interlayer electron-electron scattering. Since the intralayer electron-electron scattering does not contribute to the drag current, we concentrate on the interlayer term,

$$J^i(f_{\boldsymbol{k}})_{s_{\boldsymbol{k}} s_{\boldsymbol{k}}'} = \frac{\pi}{\hbar L^4} \sum_{\boldsymbol{k}_1 \boldsymbol{k}' \boldsymbol{k}_1'} \left| v_{|\boldsymbol{k}-\boldsymbol{k}_1|}^{(\text{pa})} \right|^2 \delta_{\boldsymbol{k}+\boldsymbol{k}', \boldsymbol{k}_1+\boldsymbol{k}_1'}$$

$$\times \left\{ \sum_{i=1}^{4} P_{s_{\boldsymbol{k}} s_{\boldsymbol{k}_1} s_{\boldsymbol{k}}'}^{(i)} A_{s_{\boldsymbol{k}'} s_{\boldsymbol{k}_1'}}^{(i)} \right.$$

$$\times \delta\left[\varepsilon_{\boldsymbol{k}_1, s_{\boldsymbol{k}_1}}^{(p)} - \varepsilon_{\boldsymbol{k}, s_{\boldsymbol{k}}'}^{(p)} + \varepsilon_{\boldsymbol{k}_1', s_{\boldsymbol{k}_1'}}^{(a)} - \varepsilon_{\boldsymbol{k}', s_{\boldsymbol{k}'}}^{(a)} \right]$$

$$+ \sum_{i=5}^{8} P_{s_{\boldsymbol{k}} s_{\boldsymbol{k}_1} s_{\boldsymbol{k}}'}^{(i)} A_{s_{\boldsymbol{k}'} s_{\boldsymbol{k}_1'}}^{(i)}$$

$$\left. \times \delta\left[\varepsilon_{\boldsymbol{k}_1, s_{\boldsymbol{k}_1}}^{(p)} - \varepsilon_{\boldsymbol{k}, s_{\boldsymbol{k}}}^{(p)} + \varepsilon_{\boldsymbol{k}_1', s_{\boldsymbol{k}_1'}}^{(a)} - \varepsilon_{\boldsymbol{k}', s_{\boldsymbol{k}'}}^{(a)} \right] \right\}, \quad (4)$$
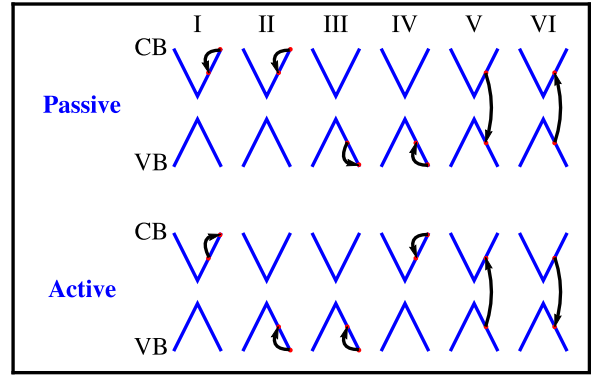
FIG. 1. Sketch of the interlayer electron-electron scattering processes that contribute to Coulomb drag. CB and VB represent the conduction and valence bands, respectively. Processes I–IV represent intraband scatterings, while interband scatterings are represented by V–VI.

where L^2 is the area of the 2D system and the quantities $A_{s_{\boldsymbol{k}'} s_{\boldsymbol{k}_1'}}^{(i)}$ and $P_{s_{\boldsymbol{k}} s_{\boldsymbol{k}_1} s_{\boldsymbol{k}}'}^{(i)}$, given explicitly in the Table I of Supplement, are functions of the occupations of the active and passive layers, respectively. The interlayer momentum transfer $\boldsymbol{q} = \boldsymbol{k} - \boldsymbol{k}_1 = \boldsymbol{k}_1' - \boldsymbol{k}'$, and $v_{|\boldsymbol{k}-\boldsymbol{k}_1|}^{(\text{pa})} = v_q^{(\text{pa})}$ is the interlayer Coulomb interaction. The interlayer electron-electron scattering processes that contribute to Coulomb drag are shown in Fig. 1, with the dominant process being I.

B. Strength of the interlayer interaction and applicability of our theory

Two parameters quantify the strength of interactions in topological insulator films and the limits of validity of the RPA. Firstly, we define an effective background dielectric constant ϵ_r. The physics of films is determined by their thickness d and the Fermi wave vector k_F [85]. We take a Bi$_2$Se$_3$ film as an example, with $\epsilon_{r, \text{Bi}_2\text{Se}_3} \approx 100$, grown on a semiconductor substrate with $\epsilon_{r,s} \approx 11$. For $k_F d \gg 1$, the film is thick, and the two surfaces are independent [88]. For the top surface, where one side is exposed to air, $\epsilon_{r, \text{top}} = (\epsilon_{r, \text{Bi}_2\text{Se}_3} + 1)/2 \approx 50$. For the bottom surface $\epsilon_{r, btm} = (\epsilon_{r, \text{Bi}_2\text{Se}_3} + \epsilon_{r,s})/2 \approx 55$. Both are independent of d. For $k_F d \ll 1$, the film is ultrathin and can be approximated as a pure 2D system, with $\epsilon_r = (1 + \epsilon_{r,s})/2 \approx 6$, also independent of d. However, since the TI bulk cannot be eliminated, $\epsilon_r \approx 6$ is an ideal lower bound. In films studied here, thick enough that there is no interlayer tunneling, implying $d > 5$ nm at the very least, ϵ_r has contributions from both the TI bulk and the semiconductor substrate, and for Bi$_2$Se$_3$ can range between 6 and 55. Two experiments have extracted $\epsilon_r \approx 30$ for relatively thick films of Bi$_2$Se$_3$ (10 nm $< d <$ 20 nm) [89,90]. Hence, ϵ_r is treated as a phenomenological parameter to be measured separately for each film. In our numerical calculations we use $\epsilon_r = 20$, which yields a Wigner-Seitz radius $r_s \ll 1$, making our RPA approach applicable to the system under study.

To obtain the dynamical screening function renormalizing the Coulomb interaction, we employ the standard procedure of solving the Dyson equation for the two-layer system in

the RPA. In this approach, $v^{(pa)}_{|\boldsymbol{k}-\boldsymbol{k}_1|}$ in Eq. (B2) becomes the dynamically screened interlayer Coulomb interaction $V(\boldsymbol{q},\omega) = \frac{v_q \mathrm{e}^{-qd}}{\epsilon(\boldsymbol{q},\omega)}$. The dielectric function of the coupled layer system is [48,50,51,54–57,63,84,91]

$$\epsilon(\boldsymbol{q},\omega) = [1 - v_q \Pi_{\mathrm{a}}(\boldsymbol{q},\omega)][1 - v_q \Pi_{\mathrm{p}}(\boldsymbol{q},\omega)]$$
$$- [v_q \mathrm{e}^{-qd}]^2 \Pi_{\mathrm{a}}(\boldsymbol{q},\omega) \Pi_{\mathrm{p}}(\boldsymbol{q},\omega), \quad (5)$$

in which the polarization function takes the form

$$\Pi_l(\boldsymbol{q},\omega) = -\frac{1}{L^2} \sum_{\boldsymbol{k}ss'} \frac{\left(f^{(l)}_{0\boldsymbol{k},s} - f^{(l)}_{0\boldsymbol{k}',s'}\right)}{\varepsilon^{(l)}_{\boldsymbol{k},s} - \varepsilon^{(l)}_{\boldsymbol{k}',s'} + \hbar\omega + i0^+} F^{ss'}_{\boldsymbol{k}\boldsymbol{k}'}, \quad (6)$$

with $f^{(l)}_{0\boldsymbol{k},s} \equiv f^{(l)}_0(\varepsilon_{\boldsymbol{k}s})$ the equilibrium Fermi distribution function and $F^{ss'}_{\boldsymbol{k}\boldsymbol{k}'} = \langle \boldsymbol{k},s,l|\boldsymbol{k}',s',l' \rangle \langle \boldsymbol{k}',s',l'|\boldsymbol{k},s,l \rangle$ is the wave-function overlap.

IV. KINETIC EQUATION FOR 3D MAGNETIC TIS

In this section we present the effective kinetic equations derived for each layer from the quantum Liouville equation. The single-particle density matrix is diagonal in the layer index $f_{\boldsymbol{k}} = \mathrm{diag}\,(f^{(a)}_{\boldsymbol{k}}, f^{(p)}_{\boldsymbol{k}})$. The scattering term $J^i(f_{\boldsymbol{k}})_{s_k s'_k}$ represents interlayer coherence: In the active layer we solve for the nonequilibrium correction to $f^{(a)}_{\boldsymbol{k}}$ [28], feed it into $J^i(f_{\boldsymbol{k}})_{s_k s'_k}$, and the result is an effective driving term for the passive layer. This then enables us to solve for the nonequilibrium to correction $f^{(p)}_{\boldsymbol{k}}$ in response to this effective driving term. The kinetic equation of the two-layer system

$$\frac{\mathrm{d}f^{(a)}_{\boldsymbol{k}}}{\mathrm{d}t} + \frac{i}{\hbar}\left[H^{(a)}_{0\boldsymbol{k}}, f^{(a)}_{\boldsymbol{k}}\right] + \hat{J}_0\left(f^{(a)}_{\boldsymbol{k}}\right) = \frac{e\boldsymbol{E}}{\hbar} \cdot \frac{\partial f^{(a)}_{0\boldsymbol{k}}}{\partial \boldsymbol{k}}, \quad (7a)$$

$$\frac{\mathrm{d}f^{(p)}_{\boldsymbol{k}}}{\mathrm{d}t} + \frac{i}{\hbar}\left[H^{(p)}_{0\boldsymbol{k}}, f^{(p)}_{\boldsymbol{k}}\right] + \hat{J}_0\left(f^{(p)}_{\boldsymbol{k}}\right) = J^i(f_{\boldsymbol{k}})_{s_k s'_k}, \quad (7b)$$

with $H^{(l)}_{0\boldsymbol{k}} = h^{(l)}_{\boldsymbol{k}} + M_l \sigma_z$ the band Hamiltonian and $f^{(l)}_{0\boldsymbol{k}}$ the equilibrium density matrix of each magnetic layer. The electron-impurity scattering integral is $\hat{J}_0(f^{(l)}_{\boldsymbol{k}}) = \langle \int_0^\infty \frac{\mathrm{d}t'}{\hbar^2}[\hat{U}, e^{-i\hat{H}t'/\hbar}[\hat{U}, \hat{f}]e^{i\hat{H}t'/\hbar}]\rangle_{\boldsymbol{k}\boldsymbol{k}}$, where $\langle\rangle$ denotes the average over impurity configurations. The above encapsulates the philosophy or our approach: To begin with, we consider an external electric field applied to the active layer, we solve for the nonequilibrium density matrix in the active layer without any reference to electron-electron scattering, and we feed the solution for the active-layer density matrix into the interlayer electron-electron scattering integral. The result of this is an electric-field dependent term that acts as a new driving term (i.e. *the drag force*) for the passive layer. We then solve for the nonequilibrium density matrix in the passive layer with this driving term. The solution thus obtained represents the nonequilibrium density matrix in the passive layer, which may be used to calculate expectation values. Specifically, its trace with the current operator yields the drag current.
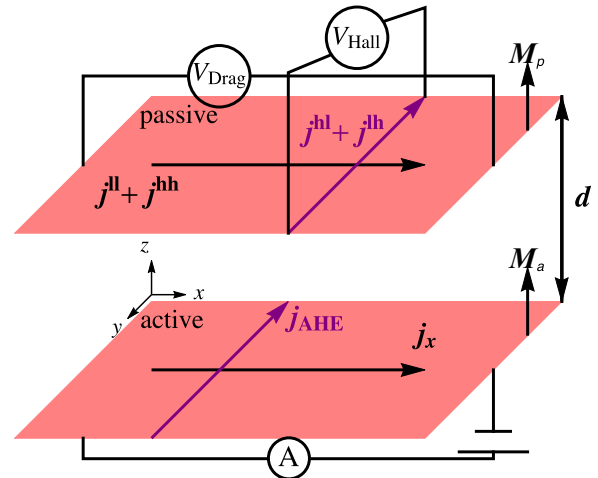
FIG. 2. Contributions to the drag current in magnetic TIs. The electric field $\parallel \hat{\boldsymbol{x}}$ gives rise to a longitudinal ($\boldsymbol{j}_x$) and an anomalous Hall ($\boldsymbol{j}_{\mathrm{AHE}}$) current in the active layer. In the passive layer there are four contributions to the drag currents: $\boldsymbol{j}^{\mathrm{ll}}$ is the longitudinal current dragged by $\boldsymbol{j}_x$; $\boldsymbol{j}^{\mathrm{lh}}$ is the transverse current dragged by $\boldsymbol{j}_{\mathrm{AHE}}$; $\boldsymbol{j}^{\mathrm{hl}}$ is the anomalous Hall current generated by $\boldsymbol{j}^{\mathrm{ll}}$; while $\boldsymbol{j}^{\mathrm{hh}}$ is the anomalous Hall current generated by $\boldsymbol{j}^{\mathrm{lh}}$, and it flows longitudinally. $\boldsymbol{M}_{\mathrm{a}}$ and $\boldsymbol{M}_{\mathrm{p}}$ are the magnetizations of the active and passive layers, respectively. d is the layer separation.

V. DRAG RESISTIVITY OF 3D MAGNETIC TIS

A. Contributions to the drag current

As a model example we will consider the surface states of 3D topological insulators in which an out of plane magnetization exists (but no magnetic field), hence the physics discussed will be that of 2D massive Dirac fermions. The drag current in the passive layer will have two components, namely a longitudinal component and a Hall component, which can be measured separately. Our interest lies primarily in the Hall component and in elucidating the dominant contributions to it. It is expected that the Hall drag current has contributions from (i) the longitudinal current in the active layer via a *transverse drag force*, (ii) the Hall current in the active layer, which may be termed *direct Hall drag* (Fig. 2). The aim of this work is to determine the relative magnitude of these distinct contributions and to identify the dominant contribution to the anomalous Hall drag response. Aside from technical considerations, the primary reason for adopting such a conceptual decomposition of the drag response is the fact that the different contributions to the Hall drag current have different physical origins. Contribution (i) represents straightforward longitudinal charge transport in the presence of impurities and other scattering mechanisms. Contribution (ii) is topological: the anomalous Hall effect in Dirac fermion systems is predominantly driven by a topological term originating in the Berry curvature associated with the band structure. The Hall drag current stemming from the *transverse drag force* of (i) in effect comes from the standard longitudinal drag current: if this turns out to dominate the Hall drag response it implies that there is no Hall drag *per se* in anomalous Hall systems, rather the measured Hall drag current is simply the anomalous Hall response to the longitudinal drag force. It would imply that the topological

terms leading to the anomalous Hall effect in the active layer do not yield a drag current in the passive layer.

We consider separately the four contributions to the drag current, corresponding to the picture presented in Fig. 2 and in the introduction. The electric field $\parallel \hat{x}$ gives rise to a longitudinal (j_x) and an anomalous Hall (j_{AHE}) current in the active layer. In the passive layer the four contributions to the drag current are: j^{ll} is the longitudinal current dragged by j_x; j^{lh} is the transverse current dragged by j_{AHE}; j^{hl} is the anomalous Hall current generated by j^{ll}; while j^{hh} is the anomalous Hall current generated by j^{lh}, and it flows longitudinally. Referring to the layer index $^{(l)}$, we write $f_k^{(l)} = n_k^{(l)}\mathbb{1} + S_k^{(l)}$, with $S_k^{(l)}$ a 2×2 Hermitian matrix which can be decomposed in terms of the Pauli spin matrices. We project the vector $\boldsymbol{\sigma}$ of Pauli spin matrices as $\sigma_{k,\parallel} = \boldsymbol{\sigma} \cdot \hat{\boldsymbol{\Omega}}_k$, $\sigma_{k,k} = \boldsymbol{\sigma} \cdot \hat{\boldsymbol{k}}$ and $\sigma_{k,z_{\text{eff}}} = \boldsymbol{\sigma} \cdot \hat{z}_{\text{eff}}$. Note that $\sigma_{k,\parallel}$ commutes with $H_{0k}^{(l)}$, while $\sigma_{k,k}$ and $\sigma_{k,z_{\text{eff}}}$ do not, hence we use $\perp$ to refer to vectors in the plane spanned by $\hat{\boldsymbol{k}}$ and $\hat{z}_{\text{eff}}$. We project $S_k^{(l)}$ onto three directions with $S_{k,\parallel}^{(l)} = \frac{1}{2} s_{k,\parallel} \sigma_{k,\parallel}$, $S_{k,k}^{(l)} = \frac{1}{2} s_{k,k} \sigma_{k,k}$ and $S_{k,z_{\text{eff}}}^{(l)} = \frac{1}{2} s_{k,z_{\text{eff}}} \sigma_{k,z_{\text{eff}}}$. The kinetic equation for the passive layer is decomposed as

$$\frac{dS_{k,\parallel}^{(p)}}{dt} + P_\parallel \hat{J}_0\big(S_k^{(p)}\big) = J^i(f_k)_{\text{ll,lh}} \quad (8a)$$

$$\frac{dS_{k,\perp}^{(p)}}{dt} + \frac{i}{\hbar}\big[H_{0k}^{(p)}, S_{k,\perp}^{(p)}\big] + P_\perp \hat{J}_0\big(S_k^{(p)}\big) = J^i(f_k)_{\text{hl,hh}} \quad (8b)$$

where $J^i(f_k)_{\text{ll,lh}}, J^i(f_k)_{\text{hl,hh}}$ can be found in Appendix B. The explicit form of the impurity scattering term $P_\parallel \hat{J}_0(S_k^{(p)}), P_\perp \hat{J}(S_k^{(p)})$ together with the solutions for the terms $S_{k,\parallel}^{(a)}, S_{k,\perp}^{(a)}$ can be found in Ref. [28]. The drag current can be expressed as $j = \text{tr}(\hat{j} S_k^{(p)})$, where $\hat{j}$ is the current operator.

B. Toy model explanation of the vanishing of the topological contribution to drag

We shall show below (Sec. V C) that the anomalous Hall current in the active layer does not generate a drag current at all in the passive layer. Before presenting the full calculation we would like to demonstrate, using a toy model, that this vanishing can be understood based on fundamental physical considerations, and for this purpose we wish to focus on the active layer and on the origins of the anomalous Hall effect.

We have divided the density matrix of the active layer as $f_k^{(a)} = n_k^{(a)}\mathbb{1} + S_{k,\parallel}^{(a)} + S_{k,\perp}^{(a)}$. The first two terms, $n_k^{(a)}\mathbb{1}$ and $S_{k,\parallel}^{(a)}$, commute with the band Hamiltonian, and represent the fraction of carriers that are in eigenstates. The term $n_k^{(a)}\mathbb{1}$ represents the charge density while $S_{k,\parallel}^{(a)}$ is the spin density. When an electric field is applied the Fermi surface is shifted and the charge and spin densities acquire nonequilibrium corrections, which are contained in $n_k^{(a)}\mathbb{1}$ and $S_{k,\parallel}^{(a)}$. If the driving term due to the electric field is denoted by D_k, we may make the same decomposition and write $D_k = D_{k,n}\mathbb{1} + D_{k,\parallel} + D_{k,\perp}$. Very crudely, we may define a single scattering time τ, in which case it is qualitatively true that

$$\begin{aligned} n_k^{(a)} &\approx D_{k,n}\tau \\ S_{k,\parallel}^{(a)} &\approx D_{k,\parallel}\tau. \end{aligned} \quad (9)$$

The τ dependence of these terms makes it immediately obvious that they are associated with the Drude conductivity. These corrections due to the fraction of carriers in eigenstates are the main terms responsible for the longitudinal conductivity (in topological insulators both the charge and spin densities must be considered when calculating the current, due to the spin-charge coupling contained in the spin-orbit interaction). When these are fed into Eq. (4) they lead to the standard longitudinal Coulomb drag current.

The term $S_{k,\perp}^{(a)}$ is associated with interband coherence, or, in the notation used here, with spin/pseudospin precession/rotations. In the same toy-model language used above $S_{k,\perp}^{(a)}$ may be written approximately as

$$S_{k,\perp}^{(a)} = \frac{1}{2} \boldsymbol{\sigma} \cdot \left(\frac{\hat{\boldsymbol{\Omega}}_k \times \boldsymbol{D}_{k,\perp}}{\Omega_k}\right), \quad (10)$$

where we have used the notation $D_{k,\perp} = (1/2)\boldsymbol{\sigma} \cdot \boldsymbol{D}_{k,\perp}$ in keeping with the notation introduced above. It is this part of the density matrix that contains the topological Berry curvature terms appearing in transport.

The anomalous Hall effect is contained in $S_{k,\perp}^{(a)}$. The presence of the cross product in Eq. (10) makes manifest the fact that this term in the density matrix stems from spin/pseudospin rotations, or alternatively coherence between eigenstates. This term does *not* represent a change in the charge/spin densities. Moreover, since $\boldsymbol{\Omega}_k$ is odd in $\boldsymbol{k}$ this term has a different angular structure from $n_k^{(a)}\mathbb{1}$ and $S_{k,\parallel}^{(a)}$. We shall see below that this angular structure causes the contribution of this term to Coulomb drag to vanish identically.

C. Drag resistivity
1. j^{ll}

The longitudinal drag conductivity σ_D^{xx} was studied in detail in many publications [37,48,50,51,54–57,63,84,91,92]. We are able to reproduce the general result

$$\sigma_D^{xx} = \frac{e^2\beta}{16\pi} \sum_q \int d\omega \frac{|v_q^{(pa)}|^2 \text{Im}\chi_a(\boldsymbol{q},\omega)\text{Im}\chi_p(\boldsymbol{q},\omega)}{\sinh^2 \frac{\beta\hbar\omega}{2}}. \quad (11)$$

where $\text{Im}\chi_l(\boldsymbol{q},\omega)$ is the imaginary part of nonlinear susceptibility and $\beta = \frac{1}{k_B T}$. In the regime $M_{a,p} \ll \varepsilon_F$, which is applicable to all samples studied experimentally. It has been shown that the drag problem reduces to the calculation of the nonlinear susceptibility of the system [48,51,56,63–65] which we detail in Appendix A.

2. j^{hl}

One of the transverse drag j^{hl} can be obtained by solving Eq. (8b), where the vertex correction from $P_\perp \hat{J}(S_k^{(p)})$ is neglected.

$$\begin{aligned} j^{hl} = \frac{e^2\beta\pi}{4\hbar L^2} \sum_{k,q} \int d\omega \frac{|v_q^{(pa)}|^2}{\sinh^2\frac{\beta\hbar\omega}{2}} \delta\big[\varepsilon_{k_1,+}^{(p)} - \varepsilon_{k,+}^{(p)} + \hbar\omega\big] \\ \times \big(f_{0k,+}^{(p)} - f_{0k_1,+}^{(p)}\big)\boldsymbol{E}_a \cdot \text{Im}\chi_a^{++}(\boldsymbol{q},\omega) \\ \times \frac{Aa_k b_k}{\Omega_k}(\hat{\boldsymbol{\theta}}_1 - \hat{\boldsymbol{\theta}}). \end{aligned} \quad (12)$$

Equation (12) is used to calculate the anomalous Hall resistivity. It can be written as a function of the Berry curvature of the passive layer, the occupation numbers ($f_{0\boldsymbol{k},+}^{(p)} - f_{0\boldsymbol{k}_1,+}^{(p)}$), and an effective driving term due to the electric field and interlayer electron-electron scattering. In order to calculate the

anomalous Hall drag coefficient, the 4×4 conductance matrix has to be inverted. Keeping the leading-order terms in the interlayer interaction and the first-order terms in the magnetization, we have $\rho_{\mathrm{D}}^{yx} \approx \frac{\sigma_{\mathrm{pa}}^{yx}}{\sigma_{\mathrm{aa}}^{xx}\sigma_{\mathrm{pp}}^{xx}}$. σ_{aa}^{xx} and σ_{pp}^{xx} are the longitudinal conductivities of the active and passive layers, respectively.

3. $\boldsymbol{j}^{\mathrm{lh}}$

Next we calculate $\boldsymbol{j}^{\mathrm{lh}}$ in the steady state. The contribution $\boldsymbol{j}^{\mathrm{lh,bare}}$ stems from the band Hamiltonian

$$\boldsymbol{j}^{\mathrm{lh,bare}} = -\frac{e^2\pi}{16\hbar L^2} \int_{-\infty}^{+\infty} \mathrm{d}\omega \sum_{\boldsymbol{k}'\boldsymbol{q}} \frac{\left|v_q^{(pa)}\right|^2}{4\sinh^2\frac{\beta\hbar\omega}{2}} \frac{\boldsymbol{E}_a a_{k'}^2 b_{k'}}{\Omega_{k'}k'} \cdot (\hat{\boldsymbol{\theta}}' - \hat{\boldsymbol{\theta}}_1')\mathrm{Im}\chi_{\mathrm{p}}^{++}(\boldsymbol{q},\omega)$$

$$\times \left\{\left(1 - f_{0\boldsymbol{k}',+}^{(a)}\right)(1 - e^{-\beta\hbar\omega})\delta\left[\varepsilon_{k_1',+}^{(a)} - \varepsilon_{k',+}^{(a)} + \hbar\omega\right] + \left(1 - f_{0\boldsymbol{k}',+}^{(a)}\right)(1 - e^{\beta\hbar\omega})\delta\left[\varepsilon_{k_1',+}^{(a)} - \varepsilon_{k',+}^{(a)} - \hbar\omega\right]\right\} \quad (13)$$

while $\boldsymbol{j}^{\mathrm{lh},vtx}$ stems from the vertex correction to the anomalous Hall current in the active layer

$$\boldsymbol{j}^{\mathrm{lh},vtx} = -\frac{e^2\beta\pi}{\hbar 8 L^2} \int_{-\infty}^{+\infty} \mathrm{d}\omega \sum_{\boldsymbol{k}'\boldsymbol{q}} \frac{\left|v_q^{(pa)}\right|^2}{4\sinh^2\frac{\beta\hbar\omega}{2}} \frac{a_{k'}b_{k'}\tau^{(a)}}{\Omega_{k'}\tau_c} \boldsymbol{E}_a \cdot (\hat{\boldsymbol{\theta}}' - \hat{\boldsymbol{\theta}}_1')\mathrm{Im}\chi_{\mathrm{p}}^{++}(\boldsymbol{q},\omega)$$

$$\times \left\{\left[2\left(f_{0\boldsymbol{k}',+}^{(a)}\right)^2 - \left(f_{0\boldsymbol{k}',+}^{(a)}\right)^3 - f_{0\boldsymbol{k}',+}^{(a)}f_{0\boldsymbol{k}_1,+}^{(a)}\right](1 - e^{\beta\hbar\omega})v_{k'}\delta\left[\varepsilon_{k_1',+}^{(a)} - \varepsilon_{k',+}^{(a)} - \hbar\omega\right]\right.$$

$$\left. + \left[2\left(f_{0\boldsymbol{k}',+}^{(a)}\right)^2 - \left(f_{0\boldsymbol{k}',+}^{(a)}\right)^3 - f_{0\boldsymbol{k}',+}^{(a)}f_{0\boldsymbol{k}_1,+}^{(a)}\right](1 - e^{-\beta\hbar\omega})v_{k'}\delta\left[\varepsilon_{k_1',+}^{(a)} - \varepsilon_{k',+}^{(a)} + \hbar\omega\right]\right\}. \quad (14)$$

We have found that the two terms in $\{\cdots\}$ cancel out after performing the variable change ω to $-\omega$, which means that $\boldsymbol{j}^{\mathrm{lh}} = \boldsymbol{j}^{\mathrm{lh,bare}} + \boldsymbol{j}^{\mathrm{lh},vtx} = 0$, as expected based on the discussion in Sec. V B.

4. $\boldsymbol{j}^{\mathrm{hh}}$

Finally we calculate $\boldsymbol{j}^{\mathrm{hh}}$ in Fig. 2:

$$\boldsymbol{j}^{\mathrm{hh,I}} = \frac{e^2\pi}{\hbar L^4} \int \mathrm{d}\omega \sum_{\boldsymbol{k}\boldsymbol{k}'\boldsymbol{q}} \left|v_q^{(pa)}\right|^2 \frac{AEa_{k'}}{2\Omega_{k'}k'} \frac{f(\gamma)}{\hbar\Omega_k} \left(f_{\boldsymbol{k},+}^{(p)} - f_{\boldsymbol{k}_1,+}^{(p)}\right)\delta\left[\varepsilon_{k_1',+}^{(a)} - \varepsilon_{k',+}^{(a)} - \hbar\omega\right]\delta\left[\varepsilon_{k_1,+}^{(p)} - \varepsilon_{k,+}^{(p)} + \hbar\omega\right]$$

$$\times \left\{\sin\theta' \frac{1 - f_{0\boldsymbol{k}_1,+}^{(a)}}{1 - e^{\beta\hbar\omega}} - \frac{1 - f_{0\boldsymbol{k}',+}^{(a)}}{1 - e^{-\beta\hbar\omega}}\sin\theta_1'\right\}\hat{\boldsymbol{\theta}}. \quad (15)$$

where the term $\propto b_k^2$ has been omitted. Here $f(\gamma) = -\frac{a_{k'}a_k}{4}\sin(\theta_1 - \theta)\sin(\theta' - \theta_1')$ and $f_{0\boldsymbol{k},+}^{(a)} \equiv f_{0\varepsilon_k,+}^{(a)}$. Integrating over the angles of the wave vectors $\boldsymbol{k}', \boldsymbol{k}$ yields $\boldsymbol{j}^{\mathrm{hh}} = 0$.

VI. DISCUSSION

A. Contributions to the drag resistivity

We have directly calculated the anomalous Hall drag resistivity ρ_{D}^{yx} according to the procedure outlined above. We have found that $\boldsymbol{j}^{\mathrm{lh}}$ and $\boldsymbol{j}^{\mathrm{hh}}$ (Fig. 2) vanish identically, implying that the anomalous Hall current in the (doped) active layer does not generate a corresponding drag current in the passive layer.

We analyze the parameter dependence of ρ_{D}^{yx} in Figs. 3 and 4. The relationship between ρ_{D}^{yx} and the magnetization of the passive layer is illustrated in Fig. 3. There is an upward trend at small magnetizations followed by a relatively slow decrease at larger values of M_{p}. The trend can be understood as follows. For $M_{\mathrm{p}} \ll Ak_{\mathrm{F}}$ one may expand Eq. (12) in M_{p}, which

reveals that the current increases nearly linearly with M_{p}. In the opposite limit in which $M_{\mathrm{p}} \gg Ak_{\mathrm{F}}$ [93], the anomalous Hall current vanishes, since the effect of spin-orbit coupling (chirality), which scales with k_{F}, becomes negligible. In fact at large M_{p} one may expand the band energies in Ak, with the leading k-dependent term scaling as k^2, which suggests the system in this limit behaves as a regular, nonmagnetic 2DEG. This explains the slow downward trend with increasing M_{p} and hence the presence of the peak as a function of M_{p}. At larger electron densities the peak occurs at stronger values of the magnetization, since higher electron densities imply higher values of Ak_{F}, increasing the effect of chirality at the expense of the magnetization. TI magnetizations have been measured by superconducting quantum interference device
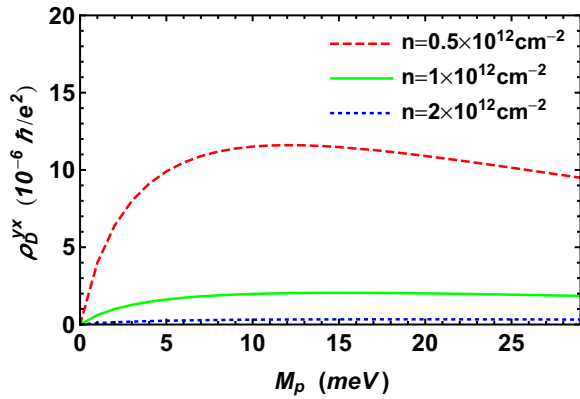
FIG. 3. Magnetization dependence of $\rho_{\rm D}^{yx}$ with $T = 5$ K, $d = 10$ nm, dielectric constant $\epsilon_r = 20$, $A = 4.1$ eV Å, and transport time $\tau_l \approx 0.1$ ps.

magnetometers [12,94]. Because the momentum scattering time is in principle known from the longitudinal conductivity of each layer [17,95], the trend exhibited by $\rho_{\rm D}^{yx}$ as a function of the magnetization $M_{\rm p}$ can be verified experimentally.

We examine the dependence of the anomalous Hall drag resistivity on additional experimentally measurable parameters. In Fig. 4(a) the electron density dependence of $\rho_{\rm D}^{yx}$ for interlayer separations $d = 20,40$ nm is shown. Compared with the longitudinal drag resistivity, the anomalous Hall drag resistivity has a weaker dependence on electron density. As compared with the longitudinal drag resistivity, the group velocity appearing in the susceptibility of the passive layer is replaced by the Berry curvature, leading to a weaker density dependence, yet no topological contribution. Next, Fig. 4(b) illustrates the temperature dependence of $\rho_{\rm D}^{yx}$ for separations $d = 10,20,40$ nm. We find that, much like $\rho_{\rm D}^{xx}$, $\rho_{\rm D}^{yx}$ also increases nearly quadratically with temperature. The T^2 dependence stems from the allowed phase space for electron-electron scattering at low temperature and is expected for any interaction strength between the top and bottom layers of TIs, provided the carriers can be described using a Fermi liquid picture. Moreover, due to the absence of backscattering in TIs there is no correction logarithmic in temperature. Fig. 4(c) presents the layer separation dependence of $\rho_{\rm D}^{yx}$ for $n = 1 \times 10^{12}$ cm^{-2}, 2×10^{12} cm^{-2}, and 3×10^{12} cm^{-2}.

Experimentally, for TI films in the large-surface limit, nontopological contributions from the bulk and the side surface are negligible [96], and we expect the effects described in this work to be observable. Aside from commonly used materials such as Bi$_2$Se$_3$ and Bi$_2$Te$_3$, a small-gap three-dimensional TI has also been identified in strained HgTe. The TI surface states in this material are, however, spatially extended and could be peaked quite far from the wide quantum well edges, reducing the effective 2D layer separation [85].

Our results are also applicable to Rashba 2DEGs, though measuring a strong anomalous Hall effect [97] can be challenging. A sizable fraction of the conductivity quantum is obtained if the two Rashba subbands experience a large magnetization splitting and $\varepsilon_{\rm F}$ lies in the bottom subband, but that is challenging experimentally. When $\varepsilon_{\rm F} \gg M_l$ the effect vanishes altogether.
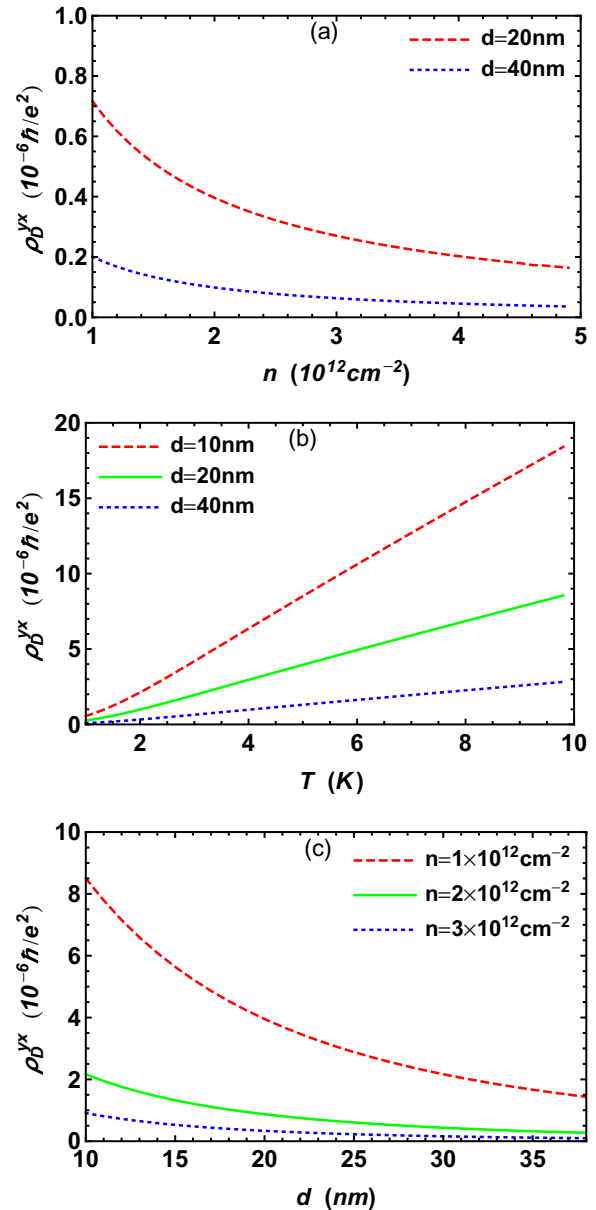
FIG. 4. (a) Electron density dependence at $T = 5$ K, (b) Temperature dependence with $n = 10^{12}$ cm^{-2}, (c) Layer separation dependence at $T = 5$ K. $M_{\rm p} = 10$ meV, dielectric constant $\epsilon_r = 20$, $A = 4.1$ eV Å, and transport time $\tau_l \approx 0.1$ ps.

B. Beyond topological insulators

Massive Dirac fermions are also found in graphene with a staggered sublattice potential and MoS$_2$ thin films where inversion symmetry is broken. The band Hamiltonian for a single layer is given by $H_{0k}^{(l)} = at(\tau k_x \sigma_x + k_y \sigma_y) + \frac{\Delta}{2} \sigma_z$ with $\tau = \pm 1$ the valley index, where a is the lattice constant, t is the effective hopping integral, and Δ is the energy gap. These Dresselhaus-like Hamiltonians can be directly mapped onto the Rashba Hamiltonian considered in this work [98]. The longitudinal drag current is identical for both TIs and other massive Dirac fermion systems, because the physical mechanism behind the longitudinal drag phenomenon is a result of rectification by the passive layer of the fluctuating

electric field generated by the active layer. However, when inversion symmetry is broken in a 2D hexagonal lattice, a pair of valleys which are time reversal of each other are distinguishable by their opposite values of magnetic moment and Berry curvature. Therefore, there will be no transverse drag current in graphene or MoS_2 with broken inversion symmetry because the Berry curvatures have opposite signs in the opposite valleys. In a Dirac semimetal, each Dirac point is fourfold degenerate and can be viewed as consisting of two Weyl nodes with opposite chiralities. Consequently, transverse drag currents also vanish in Dirac semimetals. At small magnetizations the longitudinal drag currents in these materials will be independent of the magnetizations of either layer.

C. Alternative picture of the undoped system: Absence of Coulomb drag between helical edge states

The effective two-dimensional model we have used throughout this work predicts that in the special case of the quantum anomalous Hall effect, when the system is undoped, the surface conduction band is empty, and the chemical potential lies in the magnetization gap, the drag current is identically zero. In the previous section we have discussed above the physical interpretation of this result that emerges from our effective two-dimensional picture. It is known, however, that the quantum anomalous Hall effect is associated with a set of chiral edge modes which are well defined at zero doping (and only then). In this subsection we demonstrate that an effective one-dimensional model for the edge modes at zero doping yields the same result as the two-dimensional model, and gives additional physical insight.

To this end we consider the broader case of Coulomb drag between two identical quantum spin-Hall systems, each with one Kramers pair on its edge. A current I_1 is driven along the upper edge of the lower quantum spin-Hall system and through electron-electron interactions a voltage V_2 is induced in the lower edge of the upper quantum spin-Hall system. Each quantum spin-Hall edge state can be described by Hamiltonian $H_k = Ak_x\sigma_z$, and the edge dispersion is $\epsilon_k^\pm = \pm Ak_x$ (Fig. 5). Hence the impurity scattering term becomes

$$P_\parallel \hat{J}\big(f_{\boldsymbol{k}_\parallel}^{(l)}\big) = \frac{n_i}{\pi\hbar A} \int dk_x' |\overline{U}_{\boldsymbol{k}\boldsymbol{k}'}|^2 \big(f_{\boldsymbol{k}_\parallel}^{(l)} - f_{\boldsymbol{k}_\parallel'}^{(l)}\big)\delta(k_x - k_x')\sigma_z,$$

(16)

where $\boldsymbol{k} = k_x\hat{\boldsymbol{e}}_x$ for the 1D case and $P_\parallel\hat{J}(f_{\boldsymbol{k}_\parallel}^{(l)}) = 0$. In the meantime, the direct interlayer electron-electron scattering term of Eq. (B2) becomes

$$J^i(f_{\boldsymbol{k}})_{s_k} = -\frac{2\pi}{\hbar}\sum_{\boldsymbol{k}\boldsymbol{k}'}\big|v_{|\boldsymbol{k}-\boldsymbol{k}_1|}^{(\mathrm{pa})}\big|^2 F_{s_k s_{k_1}}^{(\mathrm{p})} F_{s_{k'} s_{k_1'}}^{(\mathrm{a})}$$

$$\times \delta\big[\varepsilon_{k_1,s_{k_1}}^{(\mathrm{p})} - \varepsilon_{k,s_k}^{(\mathrm{p})} + \varepsilon_{k_1',s_{k_1'}}^{(\mathrm{a})} - \varepsilon_{k',s_{k'}}^{(\mathrm{a})}\big]$$

$$\times \big\{ f_{\boldsymbol{k},s_k}^{(\mathrm{p})}\big[1 - f_{\boldsymbol{k}_1,s_{k_1}}^{(\mathrm{p})}\big] f_{\boldsymbol{k}',s_{k'}}^{(\mathrm{a})}\big[1 - f_{\boldsymbol{k}_1',s_{k_1'}}^{(\mathrm{a})}\big]$$

$$- \big[1 - f_{\boldsymbol{k},s_k}^{(\mathrm{p})}\big] f_{\boldsymbol{k}_1,s_{k_1}}^{(\mathrm{p})}\big[1 - f_{\boldsymbol{k}',s_{k'}}^{(\mathrm{a})}\big] f_{\boldsymbol{k}_1',s_{k_1'}}^{(\mathrm{a})} \big\}. \quad (17)$$

If the distribution function is the equilibrium one, $J^i(f_{\boldsymbol{k}})_{s_k} = 0$. In the QSH 1D case, the wave function overlap $F_{s_k s_{k_1}}^{(l)} =$
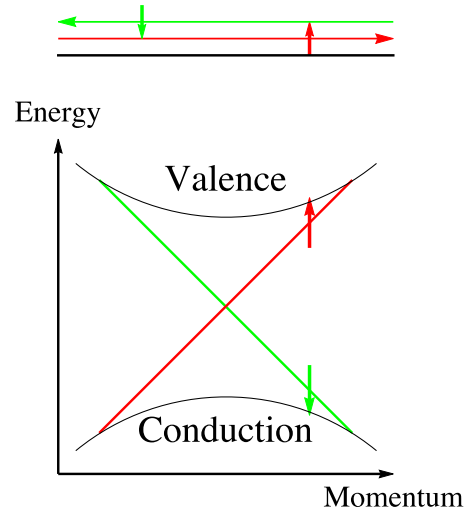
FIG. 5. A pair of helical edge states travel along the edge of a 2D topological insulator with the gapless Dirac dispersion.

1 with $s_k = s_{k_1}$ and $F_{s_k s_{k_1}}^{(l)} = 0$ with $s_k \neq s_{k_1}$. We found $J^i(f_{\boldsymbol{k}})_{s_k} = 0$. Because the spectrum is linear there is no contribution to the drag from forward scattering, and backscattering is forbidden by time-reversal symmetry [42]. Hence the Coulomb drag between two identical chiral quantum spin-Hall systems is identically zero. These results are in qualitative agreement with the work of Zyuzin and Fiete [42].

The argument presented here that chiral edge states do not give rise to drag is general and applies just as well to the Hall conductivity as to the longitudinal conductivity. The key physics is the absence of backscattering. In chiral quantum spin-Hall systems the drag current is zero because backscattering is forbidden by the linear Dirac-like dispersion. In this sense quantum anomalous-Hall systems can be regarded as a special case of quantum spin-Hall systems: They have only one state on each edge, rather than a Kramers pair. So even if backscattering were allowed by the quasiparticle dispersion there would be no states to backscatter into. Hence the drag current in quantum anomalous-Hall systems is identically zero. Yet the edge states are poorly defined at high doping, $\varepsilon_\mathrm{F}\tau_l/\hbar \gg 1$, which is the focus of this work. In addition, the Dirac fermions studied here live in TIs, which have only one shared edge between the top and bottom surfaces, making it tricky to describe thicker samples using an edge state model. In fact, at zero doping, the TI drag experiment is not well defined, since in that parameter regime leakage into the sidewall states is unavoidable.

VII. CONCLUSIONS

We have studied Coulomb drag of massive Dirac fermions, demonstrating that the drag due to the topological terms on the active surface vanishes. This is explained by the fact that the anomalous Hall current due to the topological terms in the active layer arises from the Berry phase acquired through the rearrangement of carriers among spin-momentum locked states: It is not associated with a change in the charge density (a shift in the Fermi surface) and thus cannot lead to Coulomb drag. Consequently the only contribution to anomalous Hall

TABLE I. $A^{(i)}$ and $P^{(i)}$

$$P^{(1)}_{s_k s_{k_1} s'_k} = -\langle s_k | s_{k_1}\rangle\big[1 - f^{(\mathrm{p})}_{0k_1, s_{k_1}}\big]\langle s_{k_1}|s'_k\rangle f^{(\mathrm{p})}_{0k, s'_k}$$

$$P^{(2)}_{s_k s_{k_1} s'_k} = \langle s_k | s_{k_1}\rangle f^{(\mathrm{p})}_{0k_1, s_{k_1}}\langle s_{k_1}|s'_k\rangle\big[1 - f^{(\mathrm{p})}_{0k, s'_k}\big]$$

$$P^{(3)}_{s_k s_{k_1} s'_k} = P^{(8)}_{s_k s_{k_1} s'_k} = -\langle s_k | s_{k_1}\rangle f^{(\mathrm{p})}_{0k_1, s_{k_1}}\langle s_{k_1}|s'_k\rangle$$

$$P^{(4)}_{s_k s_{k_1} s'_k} = \langle s_k | s_{k_1}\rangle\langle s_{k_1}|s'_k\rangle f^{(\mathrm{p})}_{0k, s'_k}$$

$$P^{(5)}_{s_k s_{k_1} s'_k} = \big[1 - f^{(\mathrm{p})}_{0k, s_k}\big]\langle s_k | s_{k_1}\rangle f^{(\mathrm{p})}_{0k_1, s_{k_1}}\langle s_{k_1}|s'_k\rangle$$

$$P^{(6)}_{s_k s_{k_1} s'_k} = -f^{(\mathrm{p})}_{0k, s_k}\langle s_k | s_{k_1}\rangle\big[1 - f^{(\mathrm{p})}_{0k_1, s_{k_1}}\big]\langle s_{k_1}|s'_k\rangle$$

$$P^{(7)}_{s_k s_{k_1} s'_k} = f^{(\mathrm{p})}_{0k, s_k}\langle s_k | s_{k_1}\rangle\langle s_{k_1}|s'_k\rangle$$

$$A^{(1)}_{s_{k'} s_{k'_1}} = \sum_{\varsigma_{k'}} A^{(1)}_{s_{k'} s_{k'_1} \varsigma_{k'}}, \qquad A^{(1)}_{s_{k'} s_{k'_1} \varsigma_{k'}} = \langle s_{k'} | s_{k'_1}\rangle\langle s_{k'_1}|\varsigma_{k'}\rangle f^{(\mathrm{a})}_{k', \varsigma_{k'} s_{k'}}$$

$$A^{(2)}_{s_{k'} s_{k'_1}} = \sum_{\varsigma_{k'}} A^{(2)}_{s_{k'} s_{k'_1} \varsigma_{k'}}, \qquad A^{(2)}_{s_{k'} s_{k'_1} \varsigma_{k'}} = \langle s_{k'} | s_{k'_1}\rangle f^{(\mathrm{a})}_{k'_1, s_{k'_1} \varsigma_{k'}}\langle \varsigma_{k'}|s_{k'}\rangle$$

$$A^{(3)}_{s_{k'} s_{k'_1} \varsigma_{k'_1} \varsigma_{k'}} = A^{(4)}_{s_{k'} s_{k'_1} \varsigma_{k'_1} \varsigma_{k'}} = \langle s_{k'} | s_{k'_1}\rangle f^{(\mathrm{a})}_{k'_1, s_{k'_1} \varsigma_{k'_1}}\langle \varsigma_{k'_1}|\varsigma_{k'}\rangle f^{(\mathrm{a})}_{k', \varsigma_{k'} s_{k'}}$$

$$A^{(5)}_{s_{k'} s_{k'_1}} = \sum_{\varsigma_{k'_1}} A^{(5)}_{s_{k'} s_{k'_1} \varsigma_{k'_1}}, \qquad A^{(5)}_{s_{k'} s_{k'_1} \varsigma_{k'_1}} = \langle s_{k'} | \varsigma_{k'}\rangle f^{(\mathrm{a})}_{k'_1, s_{k'_1} \varsigma_{k'_1}}\langle s_{k'_1}|s_{k'}\rangle$$

$$A^{(6)}_{s_{k'} s_{k'_1}} = \sum_{\varsigma_{k'}} A^{(6)}_{s_{k'} s_{k'_1} \varsigma_{k'}}, \qquad A^{(6)}_{s_{k'} s_{k'_1} \varsigma_{k'}} = \langle \varsigma_{k'} | s_{k'_1}\rangle\langle s_{k'_1}|s_{k'}\rangle f^{(\mathrm{a})}_{k', s_{k'} \varsigma_{k'}}$$

$$A^{(7)}_{s_{k'} s_{k'_1} \varsigma_{k'_1} \varsigma_{k'}} = A^{(8)}_{s_{k'} s_{k'_1} \varsigma_{k'_1} \varsigma_{k'}} = \langle s_{k'_1} | s_{k'}\rangle f^{(\mathrm{a})}_{k', s_{k'} \varsigma_{k'}}\langle \varsigma_{k'} | \varsigma_{k'_1}\rangle f^{(\mathrm{a})}_{k'_1, \varsigma_{k'_1} s_{k'_1}}$$

drag comes from the anomalous Hall current generated by the transverse drag force experienced by the passive layer. The transverse drag current has a nonmonotonic dependence on the magnetization of the passive layer, exhibiting a peak that becomes pronounced at lower densities.

APPENDIX A: NONLINEAR SUSCEPTIBILITY AND POLARIZATION

In special cases when the intralayer electron-electron correlations are absent, the nonlinear susceptibility is reduced to the product of the diffusion constant and the imaginary part of the polarization operator [48,50,51,53,55,56,63–65]. The small interlayer momentum transfer and excitation energy, i.e., $q < 2k_{\mathrm{F}}$, $\hbar\omega < Aq$ is the dominant region of polarization contributing to drag problem. So the polarization becomes

$$\Pi_l(\boldsymbol{q},\omega) = -\frac{k_{\mathrm{F}_l}}{2\pi A} + \frac{i}{16\pi A}\frac{q}{\sqrt{1 - \left(\frac{\hbar\omega}{Aq}\right)^2}}$$

$$\times\left[G_>\left(\frac{2k_{\mathrm{F}_l} - \frac{\hbar\omega}{A}}{q}\right) - G_>\left(\frac{2k_{\mathrm{F}_l} + \frac{\hbar\omega}{A}}{q}\right)\right], \quad \text{(A1)}$$

where

$$G_>\left(\frac{2k_{\mathrm{F}_l} \pm \frac{\hbar\omega}{A}}{q}\right) = \left[-\cosh^{-1}\left(\frac{2k_{\mathrm{F}_l} \pm \frac{\hbar\omega}{A}}{q}\right) + \frac{2k_{\mathrm{F}_l} \pm \frac{\hbar\omega}{A}}{q}\sqrt{\left(\frac{2k_{\mathrm{F}_l} \pm \frac{\hbar\omega}{A}}{q}\right)^2 - 1}\right]. \quad \text{(A2)}$$

For the case that the scattering time is independent on momentum, the nonlinear susceptibility is $\mathrm{Im}\chi_l(\boldsymbol{q},\omega) = \frac{\omega\tau_{\mathrm{F}_l}}{\pi A}\sqrt{1 - \left(\frac{q}{2k_{\mathrm{F}_l}}\right)^2}\hat{\boldsymbol{q}}$ with τ_{F_l} the transport time at Fermi level [48,51,55].

APPENDIX B: ELECTRON-ELECTRON SCATTERING

With definition $\{\{\hat{A}\}\} = \hat{A} - \mathrm{tr}\hat{A}$, the electron-electron operator $\hat{J}_{ee}(\hat{\rho}|t)$ is written as [86]

$$\hat{J}_{ee}(\hat{\rho}|t) = \frac{1}{\hbar^2 L^4}\sum_{\boldsymbol{q}\boldsymbol{q}_1} v_q v_{q_1}\int_0^\infty dt_1 e^{\lambda t_1}\big[e^{-i\boldsymbol{q}\cdot\boldsymbol{x}}\hat{S}(t,t_1)(\mathbb{1} - \hat{\rho}_{t_1})e^{i\boldsymbol{q}_1\cdot\boldsymbol{x}}\hat{\rho}_{t_1}\hat{S}^+(t,t_1)\{\{e^{i\boldsymbol{q}\cdot\boldsymbol{x}}\hat{S}(t,t_1)e^{-i\boldsymbol{q}_1\cdot\boldsymbol{x}}\hat{\rho}_{t_1}\hat{S}^+(t,t_1)\}\}$$

$$- \hat{S}(t,t_1)\hat{\rho}_{t_1}e^{i\boldsymbol{q}_1\cdot\boldsymbol{x}}(\mathbb{1} - \hat{\rho}_{t_1})\hat{S}^+(t,t_1)\{\{e^{i\boldsymbol{q}\cdot\boldsymbol{x}}\hat{S}(t,t_1)\hat{\rho}_{t_1}e^{-i\boldsymbol{q}_1\cdot\boldsymbol{x}}\hat{S}^+(t,t_1)\}\}$$

$$+ \hat{S}(t,t_1)[\hat{\rho}_{t_1}, e^{i\boldsymbol{q}_1\cdot\boldsymbol{x}}]\hat{S}^+(t,t_1)\{\{e^{i\boldsymbol{q}\cdot\boldsymbol{x}}\hat{S}(t,t_1)\hat{\rho}_{t_1}e^{-i\boldsymbol{q}_1\cdot\boldsymbol{x}}\hat{\rho}_{t_1}\hat{S}^+(t,t_1)\}\}\big], \quad \text{(B1)}$$

where $\hat{S}(t,t_1)$ is the time evolution operator which satisfies $\hat{S}(t,t_1) = \hat{S}^+(t_1,t)$ and $H^{(l)}_{0k}|\boldsymbol{k},s_k,l\rangle = \varepsilon^{(l)}_{ks_k}|\boldsymbol{k},s_k,l\rangle$. With $\langle \boldsymbol{k}s_k l|\hat{J}_{ee}(\hat{\rho}|t)|\boldsymbol{k}s'_k l'\rangle$, the terms containing the trace contribute to direct Coulomb interaction and the remaining terms contribute to exchange interaction. Accounting for both diagonal and off-diagonal parts of the density matrix, we arrange the interlayer electron-electron scattering matrix as

$$J^i(f_k)_{s_k s'_k} = \frac{\pi}{\hbar L^4}\sum_{\boldsymbol{k}_1 \boldsymbol{k}' \boldsymbol{k}'_1}\big|v^{(\mathrm{pa})}_{|\boldsymbol{k}-\boldsymbol{k}_1|}\big|^2\delta_{\boldsymbol{k}+\boldsymbol{k}', \boldsymbol{k}_1 + \boldsymbol{k}'_1}\bigg\{\delta\big[\varepsilon^{(\mathrm{p})}_{k_1, s_{k_1}} - \varepsilon^{(\mathrm{p})}_{k, s'_k} + \varepsilon^{(\mathrm{a})}_{k'_1, s_{k'_1}} - \varepsilon^{(\mathrm{a})}_{k', s_{k'}}\big]$$

$$\times\left(\sum_{i=1}^4 P^{(i)}_{s_k s_{k_1} s'_k} A^{(i)}_{s_{k'} s_{k'_1}}\right) + \delta\big[\varepsilon^{(\mathrm{p})}_{k_1, s_{k_1}} - \varepsilon^{(\mathrm{p})}_{k, s_k} + \varepsilon^{(\mathrm{a})}_{k'_1, s_{k'_1}} - \varepsilon^{(\mathrm{a})}_{k', s_{k'}}\big]\left(\sum_{i=5}^8 P^{(i)}_{s_k s_{k_1} s'_k} A^{(i)}_{s_{k'} s_{k'_1}}\right)\bigg\}, \quad \text{(B2)}$$

where $\boldsymbol{k}_1 - \boldsymbol{k} = \boldsymbol{k}' - \boldsymbol{k}_1' = \boldsymbol{q}$ and $J^i(f_{\boldsymbol{k}})_{-+} = [J^i(f_{\boldsymbol{k}})_{+-}]^*$. $P^{(i)}$ and $A^{(i)}$ are defined in Table I with

$$E_{\boldsymbol{k}'\boldsymbol{k}} = \begin{pmatrix} \langle \boldsymbol{k}', +, l | \boldsymbol{k}, +, l \rangle & \langle \boldsymbol{k}', +, l | \boldsymbol{k}, -, l \rangle \\ \langle \boldsymbol{k}', -, l | \boldsymbol{k}, +, l \rangle & \langle \boldsymbol{k}', -, l | \boldsymbol{k}, -, l \rangle \end{pmatrix} = \begin{pmatrix} 1 - \frac{1+b_k}{2}[1 - e^{i(\theta'-\theta)}] & a_k \frac{1-e^{i(\theta'-\theta)}}{2} \\ a_k \frac{1-e^{i(\theta'-\theta)}}{2} & 1 - \frac{1-b_k}{2}[1 - e^{i(\theta'-\theta)}] \end{pmatrix}. \tag{B3}$$

The interlayer electron-electron scattering processes allowed in Eq. (B2) are listed in the Fig. 1. The remaining 10 processes are forbidden by the law of energy conservation. Firstly, we calculate the contribution to drag currents from process I. Equation (B2) can be written as:

$$J^i(f_{\boldsymbol{k}})_{s_k s_k'} = \frac{J^i(f_{\boldsymbol{k}})_{++} + J^i(f_{\boldsymbol{k}})_{--}}{2}\mathbb{1} + \frac{J^i(f_{\boldsymbol{k}})_{++} - J^i(f_{\boldsymbol{k}})_{--}}{2}\sigma_z + \frac{J^i(f_{\boldsymbol{k}})_{-+} + J^i(f_{\boldsymbol{k}})_{+-}}{2}\sigma_x + \frac{J^i(f_{\boldsymbol{k}})_{-+} - J^i(f_{\boldsymbol{k}})_{+-}}{2i}\sigma_y, \tag{B4}$$

with $\mathbb{1}$ is 2×2 unit matrix and $\sigma_{x,y,z}$ are Pauli matrix. We should transform Eq. (B4) from eigenstates representation (ER) to that of σ_z (ordinary representation, OR) with

$$\mathrm{T} = \begin{pmatrix} -ie^{i\theta_k}\sqrt{\frac{1+b_k}{2}} & \frac{a_k}{\sqrt{2(1+b_k)}} \\ ie^{i\theta_k}\sqrt{\frac{1-b_k}{2}} & \frac{a_k}{\sqrt{2(1-b_k)}} \end{pmatrix}, \tag{B5}$$

and for any 2×2 matrix $\mathcal{M}$, $\mathcal{M}^{\mathrm{OR}} = \mathrm{T}^\dagger \cdot \mathcal{M}^{\mathrm{ER}} \cdot \mathrm{T}$. We have $\sigma_z \rightarrow \boldsymbol{\sigma} \cdot \hat{\boldsymbol{\Omega}}_{\boldsymbol{k}}, \sigma_x \rightarrow -\boldsymbol{\sigma} \cdot \hat{\boldsymbol{z}}_{\mathrm{eff}}, \sigma_y \rightarrow \boldsymbol{\sigma} \cdot \hat{\boldsymbol{k}}_{\mathrm{eff}}$. In σ_z representation, the electron-electron scattering term is divided into

$$-\frac{J^i(f_{\boldsymbol{k}})_{++} - J^i(f_{\boldsymbol{k}})_{--}}{2}\boldsymbol{\sigma} \cdot \hat{\boldsymbol{\Omega}}_{\boldsymbol{k}} = J^i(f_{\boldsymbol{k}})_{\mathrm{ll,lh}}, \quad \boldsymbol{\sigma} \cdot \hat{\boldsymbol{z}}_{\mathrm{eff}}\frac{J^i(f_{\boldsymbol{k}})_{-+} + J^i(f_{\boldsymbol{k}})_{+-}}{2} - \boldsymbol{\sigma} \cdot \hat{\boldsymbol{k}}_{\mathrm{eff}}\frac{J^i(f_{\boldsymbol{k}})_{-+} - J^i(f_{\boldsymbol{k}})_{+-}}{2i} = J^i(f_{\boldsymbol{k}})_{\mathrm{hl,hh}}. \tag{B6}$$

We write out $J^i(f_{\boldsymbol{k}})_{\mathrm{ll}}, J^i(f_{\boldsymbol{k}})_{\mathrm{lh}}, J^i(f_{\boldsymbol{k}})_{\mathrm{hl}}, J^i(f_{\boldsymbol{k}})_{\mathrm{hh}}$ after separately feeding the diagonal and off-diagonal density matrices elements of the active layer into Eq. (B2)

$$J^i(f_{\boldsymbol{k}})_{\mathrm{ll}} = \frac{e\pi}{L^4 k_{\mathrm{B}}T\hbar}\int d\omega \sum_{\boldsymbol{k}'\boldsymbol{q}} \frac{|v_q^{(pa)}|^2}{4\sinh^2\frac{\beta\hbar\omega}{2}} F_{\boldsymbol{k}\boldsymbol{k}_1}^{++} F_{\boldsymbol{k}'\boldsymbol{k}_1'}^{++} \delta[\varepsilon_{k_1,+}^{(p)} - \varepsilon_{k,+}^{(p)} + \hbar\omega]\delta[\varepsilon_{k_1',+}^{(a)} - \varepsilon_{k',+}^{(a)} - \hbar\omega]$$
$$\times [(f_{0\boldsymbol{k}_1,+}^{(p)} - f_{0\boldsymbol{k},+}^{(p)})(f_{0\boldsymbol{k}_1',+}^{(a)} - f_{0\boldsymbol{k}',+}^{(a)})]\boldsymbol{E}_a \cdot A[\tau_a(k_1')a_{k_1'}\hat{\boldsymbol{k}}_1' - \tau_a(k')a_{k'}\hat{\boldsymbol{k}}']\boldsymbol{\sigma} \cdot \hat{\boldsymbol{\Omega}}_{\boldsymbol{k}}. \tag{B7a}$$

$$J^i(f_{\boldsymbol{k}})_{\mathrm{lh}} = \frac{\pi}{2L^4}\int d\omega \sum_{\boldsymbol{k}'\boldsymbol{q}} |v_q^{(pa)}|^2 F_{\boldsymbol{k},\boldsymbol{k}_1}^{++}\frac{eEa_{k'}}{2\hbar\Omega_{k'}k'}a_{k'}b_{k'}(\sin\theta' - \sin\theta_1')\delta[\varepsilon_{k_1',+}^{(a)} - \varepsilon_{k',+}^{(a)} - \hbar\omega]$$
$$\times \{(f_{0\boldsymbol{k}',+}^{(a)} - f_{0\boldsymbol{k}',-}^{(a)})[(1 - f_{0\boldsymbol{k}_1,+}^{(p)})f_{0\boldsymbol{k},+}^{(p)} - (f_{0\boldsymbol{k},+}^{(p)} - f_{0\boldsymbol{k}_1,+}^{(p)})f_{0\boldsymbol{k}_1',+}^{(a)}]$$
$$+ [(1 - f_{0\boldsymbol{k},+}^{(p)})f_{0\boldsymbol{k}_1,+}^{(p)} + (f_{0\boldsymbol{k},+}^{(p)} - f_{0\boldsymbol{k}_1,+}^{(p)})f_{0\boldsymbol{k}',+}^{(a)}](f_{0\boldsymbol{k}_1',+}^{(a)} - f_{0\boldsymbol{k}_1',-}^{(a)})\}\delta[\varepsilon_{k_1,+}^{(p)} - \varepsilon_{k,+}^{(p)} + \hbar\omega]\boldsymbol{\sigma} \cdot \hat{\boldsymbol{\Omega}}_{\boldsymbol{k}}, \tag{B7b}$$

with $f_{0\boldsymbol{k}',-}^{(a)} = f_{0\boldsymbol{k}_1,-}^{(a)} = 1$.

$$J^i(f_{\boldsymbol{k}})_{\mathrm{hl}} = \frac{e\pi}{4k_{\mathrm{B}}TL^4}\sum_{\boldsymbol{k}'\boldsymbol{q}}\int d\omega \frac{|v_q^{(pa)}|^2}{\sinh^2\frac{\beta\hbar\omega}{2}}F_{\boldsymbol{k}'\boldsymbol{k}_1'}^{++}\delta[\varepsilon_{k_1',+}^{(a)} - \varepsilon_{k',+}^{(a)} - \hbar\omega](f_{0\boldsymbol{k}',+}^{(a)} - f_{0\boldsymbol{k}_1',+}^{(a)})\boldsymbol{E}_a \cdot [\tau_a(k')\boldsymbol{v}_{k'} - \tau_a(k_1')\boldsymbol{v}_{k_1'}]$$
$$\times \delta[\varepsilon_{k_1,+}^{(p)} - \varepsilon_{k,+}^{(p)} + \hbar\omega](f_{0\boldsymbol{k},+}^{(p)} - f_{0\boldsymbol{k}_1,+}^{(p)})\left\{ -\frac{a_k b_k}{2}[1 - \cos(\theta - \theta_1)]\boldsymbol{\sigma} \cdot \hat{\boldsymbol{z}}_{\mathrm{eff}} + i\frac{a_k}{2}\sin(\theta_1 - \theta)\boldsymbol{\sigma} \cdot \hat{\boldsymbol{k}}_{\mathrm{eff}}\right\}. \tag{B7c}$$

$$J^i(f_{\boldsymbol{k}})_{\mathrm{hh}} = \frac{\pi}{4L^4}\int d\omega \sum_{\boldsymbol{k}'\boldsymbol{q}} |v_q^{(pa)}|^2 \delta[\varepsilon_{k_1,+}^{(p)} - \varepsilon_{k,+}^{(p)} + \hbar\omega]\delta[\varepsilon_{k_1',+}^{(a)} - \varepsilon_{k',+}^{(a)} - \hbar\omega]f(\gamma)$$
$$\times \frac{eEa_{k'}}{2\hbar\Omega'k'}\{[(1 - f_{0\boldsymbol{k},+}^{(p)})f_{0\boldsymbol{k}_1,+}^{(p)} + (f_{0\boldsymbol{k},+}^{(p)} - f_{0\boldsymbol{k}_1,+}^{(p)})f_{0\boldsymbol{k}',+}^{(a)}]\sin\theta_1'(f_{0\boldsymbol{k}_1',+}^{(a)} - f_{0\boldsymbol{k}_1',-}^{(a)})$$
$$- [(1 - f_{0\boldsymbol{k}_1,+}^{(p)})f_{0\boldsymbol{k},+}^{(p)} - (f_{0\boldsymbol{k},+}^{(p)} - f_{0\boldsymbol{k}_1,+}^{(p)})f_{0\boldsymbol{k}_1',+}^{(a)}]\sin\theta'(f_{0\boldsymbol{k}',+}^{(a)} - f_{0\boldsymbol{k}',-}^{(a)})\}\boldsymbol{\sigma} \cdot \hat{\boldsymbol{z}}_{\mathrm{eff}}, \tag{B7d}$$

where $f(\gamma) = -\frac{a_{k'}a_k}{4}\sin(\theta_1 - \theta)\sin(\theta' - \theta_1')$.

[1] C. L. Kane and E. J. Mele, Phys. Rev. Lett. **95**, 226801 (2005).

[2] M. Z. Hasan and C. L. Kane, Rev. Mod. Phys. **82**, 3045 (2010).

[3] D. Xiao, G.-B. Liu, W. Feng, X. Xu, and W. Yao, Phys. Rev. Lett. **108**, 196802 (2012).

[4] A. A. Burkov and L. Balents, Phys. Rev. Lett. **107**, 127205 (2011).

[5] M. T. Edmonds, J. Hellerstedt, K. M. O'Donnell, A. Tadich, and M. S. Fuhrer, ACS Appl. Mater. Interfaces **8**, 16412 (2016).

[6] J. Hellerstedt, M. T. Edmonds, N. Ramakrishnan, C. Liu, B. Weber, A. Tadich, K. M. O'Donnell, S. Adam, and M. S. Fuhrer, Nano Lett. **16**, 3210 (2016).

[7] G. Wang, X.-G. Zhu, Y.-Y. Sun, Y.-Y. Li, T. Zhang, J. Wen, X. Chen, K. He, L.-L. Wang, X.-C. Ma *et al.*, Adv. Mater. **23**, 2929 (2011).

[8] B. Sacépé, J. B. Oostinga, J. Li, A. Ubaldini, N. J. G. Couto, E. Giannini, and A. F. Morpurgo, Nat. Commun. **2**, 575 (2011).

[9] H.-T. He, G. Wang, T. Zhang, I.-K. Sou, G. K. L. Wong, J.-N. Wang, H.-Z. Lu, S.-Q. Shen, and F.-C. Zhang, Phys. Rev. Lett. **106**, 166805 (2011).

[10] Z. Ren, A. A. Taskin, S. Sasaki, K. Segawa, and Y. Ando, Phys. Rev. B **85**, 155301 (2012).

[11] D. Kim, S. Cho, N. P. Butch, P. Syers, K. Kirshenbaum, S. Adam, J. Paglione, and M. S. Fuhrer, Nat. Phys. **8**, 459 (2012).

[12] J. Zhang, C.-Z. Chang, P. Tang, Z. Zhang, X. Feng, K. Li, L.-l. Wang, X. Chen, C. Liu, W. Duan *et al.*, Science **339**, 1582 (2013).

[13] L. Barreto, L. Khnemund, F. Edler, C. Tegenkamp, J. Mi, M. Bremholm, B. B. Iversen, C. Frydendahl, M. Bianchi, and P. Hofmann, Nano Lett. **14**, 3755 (2014).

[14] J. Tang, L.-T. Chang, X. Kou, K. Murata, E. S. Choi, M. Lang, Y. Fan, Y. Jiang, M. Montazeri, W. Jiang *et al.*, Nano Lett. **14**, 5423 (2014).

[15] D. A. Kozlov, Z. D. Kvon, E. B. Olshanetsky, N. N. Mikhailov, S. A. Dvoretsky, and D. Weiss, Phys. Rev. Lett. **112**, 196801 (2014).

[16] D. Kim, P. Syers, N. P. Butch, J. Paglione, and M. S. Fuhrer, Nat. Commun. **4**, 2040 (2013).

[17] C. Cacho, A. Crepaldi, M. Battiato, J. Braun, F. Cilento, M. Zacchigna, M. Richter, O. Heckmann, E. Springate, Y. Liu *et al.*, Phys. Rev. Lett. **114**, 097401 (2015).

[18] J. Zhang, X. Feng, Y. Xu, M. Guo, Z. Zhang, Y. Ou, Y. Feng, K. Li, H. Zhang, L. Wang *et al.*, Phys. Rev. B **91**, 075431 (2015).

[19] J. Hellerstedt, M. T. Edmonds, J. H. Chen, W. G. Cullen, C. X. Zheng, and M. S. Fuhrer, Appl. Phys. Lett. **105**, 173506 (2014).

[20] C. Kastl, C. Karnetzky, H. Karl, and A. W. Holleitner, Nat. Commun. **6**, 6617 (2015).

[21] Y. Fan, X. Kou, P. Upadhyaya, Q. Shao, L. Pan, M. Lang, X. Che, J. Tang, M. Montazeri, K. Murata *et al.*, Nat. Nano. **11**, 352 (2016).

[22] E. H. Hwang and S. Das Sarma, Phys. Rev. B **75**, 205418 (2007).

[23] J. Jung and A. H. MacDonald, Phys. Rev. B **84**, 085446 (2011).

[24] A. C. Durst, Phys. Rev. B **91**, 094519 (2015).

[25] H.-Z. Lu and S.-Q. Shen, Proc. SPIE **9167**, 91672E (2014).

[26] W. Zhang, R. Yu, H.-J. Zhang, X. Dai, and Z. Fang, New J. Phys. **12**, 065013 (2010).

[27] S. Liu, Y. Kim, L. Z. Tan, and A. M. Rappe, Nano Lett. **16**, 1663 (2016).

[28] D. Culcer and S. Das Sarma, Phys. Rev. B **83**, 245441 (2011).

[29] S. Adam, E. H. Hwang, and S. Das Sarma, Phys. Rev. B **85**, 235413 (2012).

[30] T. Yoshida, S. Fujimoto, and N. Kawakami, Phys. Rev. B **85**, 125113 (2012).

[31] S. Das Sarma and Q. Li, Phys. Rev. B **88**, 081404 (2013).

[32] W. E. Liu, H. Liu, and D. Culcer, Phys. Rev. B **89**, 195417 (2014).

[33] H.-Z. Lu and S.-Q. Shen, Phys. Rev. Lett. **112**, 146601 (2014).

[34] S. Das Sarma, E. H. Hwang, and H. Min, Phys. Rev. B **91**, 035201 (2015).

[35] I. Žutić, J. Fabian, and S. Das Sarma, Rev. Mod. Phys. **76**, 323 (2004).

[36] C. Nayak, S. H. Simon, A. Stern, M. Freedman, and S. Das Sarma, Rev. Mod. Phys. **80**, 1083 (2008).

[37] M. Pogrebinskii, Sov. Phys. Semicond. **11**, 372 (1977).

[38] B. N. Narozhny and A. Levchenko, Rev. Mod. Phys. **88**, 025003 (2016).

[39] K. Kaasbjerg and A.-P. Jauho, Phys. Rev. Lett. **116**, 196801 (2016).

[40] D. Laroche, G. Gervais, M. P. Lilly, and J. L. Reno, Science **343**, 631 (2014).

[41] A. P. Dmitriev, I. V. Gornyi, and D. G. Polyakov, Phys. Rev. B **86**, 245402 (2012).

[42] V. A. Zyuzin and G. A. Fiete, Phys. Rev. B **82**, 113305 (2010).

[43] A.-P. Jauho and H. Smith, Phys. Rev. B **47**, 4420 (1993).

[44] D. Nandi, A. D. K. Finck, J. P. Eisenstein, L. N. Pfeiffer, and K. W. West, Nature (London) **488**, 481 (2012).

[45] D. K. Efimkin and V. Galitski, Phys. Rev. Lett. **116**, 046801 (2016).

[46] I. V. Gornyi, A. G. Yashenkin, and D. V. Khveshchenko, Phys. Rev. Lett. **83**, 152 (1999).

[47] R. Pillarisetty, H. Noh, D. C. Tsui, E. P. De Poortere, E. Tutuc, and M. Shayegan, Phys. Rev. Lett. **89**, 016805 (2002).

[48] A. Kamenev and Y. Oreg, Phys. Rev. B **52**, 7516 (1995).

[49] V. Braude and A. Stern, Phys. Rev. B **64**, 115431 (2001).

[50] W.-K. Tse, Ben Yu-Kuang Hu, and S. Das Sarma, Phys. Rev. B **76**, 081401 (2007).

[51] B. Amorim and N. M. R. Peres, J. Phys.: Condens. Matter **24**, 335602 (2012).

[52] S. Kim, I. Jo, J. Nah, Z. Yao, S. K. Banerjee, and E. Tutuc, Phys. Rev. B **83**, 161401 (2011).

[53] W.-K. Tse and S. Das Sarma, Phys. Rev. B **75**, 045333 (2007).

[54] M. I. Katsnelson, Phys. Rev. B **84**, 041407 (2011).

[55] E. H. Hwang, R. Sensarma, and S. Das Sarma, Phys. Rev. B **84**, 245441 (2011).

[56] M. Carrega, T. Tudorovskiy, A. Principi, M. I. Katsnelson, and M. Polini, New J. Phys. **14**, 063033 (2012).

[57] B. N. Narozhny, M. Titov, I. V. Gornyi, and P. M. Ostrovsky, Phys. Rev. B **85**, 195421 (2012).

[58] S. Kim and E. Tutuc, Solid State Commun. **152**, 1283 (2012).

[59] R. V. Gorbachev, A. K. Geim, M. I. Katsnelson, K. S. Novoselov, T. Tudorovskiy, I. V. Grigorieva, A. H. MacDonald, S. V. Morozov, K. Watanabe, T. Taniguchi *et al.*, Nat. Phys. **8**, 896 (2012).

[60] M. Schütt, P. M. Ostrovsky, M. Titov, I. V. Gornyi, B. N. Narozhny, and A. D. Mirlin, Phys. Rev. Lett. **110**, 026601 (2013).

[61] A. Gamucci, D. Spirito, M. Carrega, B. Karmakar, A. Lombardo, M. Bruna, L. N. Pfeiffer, K. W. West, A. C. Ferrari, M. Polini *et al.*, Nat. Commun. **5**, 5824 (2014).

[62] M. Titov, R. V. Gorbachev, B. N. Narozhny, T. Tudorovskiy, M. Schütt, P. M. Ostrovsky, I. V. Gornyi, A. D. Mirlin, M. I. Katsnelson, K. S. Novoselov *et al.*, Phys. Rev. Lett. **111**, 166601 (2013).

[63] K. Flensberg, Ben Yu-Kuang Hu, A.-P. Jauho, and J. M. Kinaret, Phys. Rev. B **52**, 14761 (1995).

[64] B. N. Narozhny, I. L. Aleiner, and A. Stern, Phys. Rev. Lett. **86**, 3610 (2001).

[65] B. N. Narozhny and I. L. Aleiner, Phys. Rev. Lett. **84**, 5383 (2000).

[66] J. C. W. Song and L. S. Levitov, Phys. Rev. Lett. **111**, 126601 (2013).

[67] B. Scharf and A. Matos-Abiague, Phys. Rev. B **86**, 115425 (2012).

[68] J. C. W. Song, D. A. Abanin, and L. S. Levitov, Nano Lett. **13**, 3631 (2013).

[69] D. K. Efimkin and Y. E. Lozovik, Phys. Rev. B **88**, 235420 (2013).

[70] S. Murakami, N. Nagaosa, and S. C. Zhang, Phys. Rev. Lett. **93**, 156804 (2004).

[71] M. König, S. Wiedmann, C. Brüne, A. Roth, H. Buhmann, L. W. Molenkamp, X.-L. Qi, and S.-C. Zhang, Science **318**, 766 (2007).

[72] C.-Z. Chang, J. Zhang, X. Feng, J. Shen, Z. Zhang, M. Guo, K. Li, Y. Ou, P. Wei, L.-L. Wang *et al.*, Science **340**, 167 (2013).

[73] C.-Z. Chang, W. Zhao, D. Y. Kim, H. Zhang, B. A. Assaf, D. Heiman, S.-C. Zhang, C. Liu, M. H. W. Chan, and J. S. Moodera, Nat. Mater. **14**, 473 (2015).

[74] A. C. Mahoney, J. I. Colless, S. J. Pauka, J. M. Hornibrook, J. D. Watson, G. C. Gardner, M. J. Manfra, A. C. Doherty, and D. J. Reilly, Phys. Rev. X **7**, 011007 (2017).

[75] N. Nagaosa, J. Sinova, S. Onoda, A. H. MacDonald, and N. P. Ong, Rev. Mod. Phys. **82**, 1539 (2010).

[76] W. Yao, D. Xiao, and Q. Niu, Phys. Rev. B **77**, 235406 (2008).

[77] R. Yu, W. Zhang, H. J. Zhang, S. C. Zhang, X. Dai, and Z. Fang, Science **329**, 61 (2010).

[78] S. Ulstrup, J. C. Johannsen, F. Cilento, J. A. Miwa, A. Crepaldi, M. Zacchigna, C. Cacho, R. Chapman, E. Springate, S. Mammadov *et al.*, Phys. Rev. Lett. **112**, 257401 (2014).

[79] D. Xiao, M.-C. Chang, and Q. Niu, Rev. Mod. Phys. **82**, 1959 (2010).

[80] H.-Z. Lu, A. Zhao, and S.-Q. Shen, Phys. Rev. Lett. **111**, 146802 (2013).

[81] N. P. R. Hill, J. T. Nicholls, E. H. Linfield, M. Pepper, D. A. Ritchie, A. R. Hamilton, and G. A. C. Jones, J. Phys.: Condens. Matter **8**, L557 (1996).

[82] B. Y.-K. Hu, Physica. Scripta. **T69**, 170 (1997).

[83] N. K. Patel, E. H. Linfield, K. M. Brown, M. Pepper, D. A. Ritchie, and G. A. C. Jones, Semicond. Sci. Technol. **12**, 309 (1997).

[84] A. G. Rojo, J. Phys.: Condens. Matter **11**, R31 (1999).

[85] D. Tilahun, B. Lee, E. M. Hankiewicz, and A. H. MacDonald, Phys. Rev. Lett. **107**, 246401 (2011).

[86] F. T. Vasko and O. E. Raichev, *Quantum Kinetic Theory and Applications* (Springer, New York, 2005).

[87] D. Culcer, Phys. Rev. B **84**, 235411 (2011).

[88] T. Ando, A. B. Fowler, and F. Stern, Rev. Mod. Phys. **54**, 437 (1982).

[89] H. Beidenkopf, P. Roushan, J. Seo, L. Gorman, I. Drozdov, Y. S. Hor, R. J. Cava, and A. Yazdani, Nat. Phys. **7**, 939 (2011).

[90] D. Kim, Q. Li, P. Syers, N. P. Butch, J. Paglione, S. D. Sarma, and M. S. Fuhrer, Phys. Rev. Lett. **109**, 166801 (2012).

[91] H. Liu, W. E. Liu, and D. Culcer, Physica E **79**, 72 (2016).

[92] L. Zheng and A. H. MacDonald, Phys. Rev. B **48**, 8203 (1993).

[93] J.-i. Inoue, T. Kato, Y. Ishikawa, H. Itoh, G. E. W. Bauer, and L. W. Molenkamp, Phys. Rev. Lett. **97**, 046604 (2006).

[94] Y. S. Hor, P. Roushan, H. Beidenkopf, J. Seo, D. Qu, J. G. Checkelsky, L. A. Wray, Y. Xia, S.-Y. Xu, D. Qian *et al.*, Phys. Rev. B **81**, 195203 (2010).

[95] X. Peng, Y. Yang, R. R. P. Singh, S. Y. Savrasov, and D. Yu, Nat. Commun. **7**, 10878 (2016).

[96] T. Morimoto, A. Furusaki, and N. Nagaosa, Phys. Rev. B **92**, 085113 (2015).

[97] D. Culcer, A. H. MacDonald, and Q. Niu, Phys. Rev. B **68**, 045327 (2003).

[98] T. Wehling, A. Black-Schaffer, and A. Balatsky, Adv. Phys. **63**, 1 (2014).